

Impact Localisation of a Smart Composite Panel using Wave Velocity Propagation

S. Mahzan^{1,*}, W.J. Staszewski²

¹Faculty of Mechanical and Manufacturing Engineering
Tun Hussein Onn University of Malaysia (UTHM)
Parit Raja, Batu Pahat, 86400 Johor
Malaysia

²Department of Mechanical Engineering
University of Sheffield, Mappin Street,
Sheffield S1 3JD United Kingdom

*corresponding author sharudin@uthm.edu.my

Abstract:

The susceptibility of composite to withstand impact damage challenge the existing maintenance technologies related to damage detection. The problem of impact localisation in composite structures requires a reliable technique for impact damage detection. This paper investigates the reliability of strain data for impact damage localisation. A finite element model has been developed to simulate the impact strain wave propagation which can be used to ease the signal processing data. A series of impacts is experimentally performed on a smart composite panel instrumented with low-profile, embedded piezoceramic transducers. Two wave velocity propagation characteristics are developed using the strain data from both the simulation and experimental works. A Genetic Algorithm, together with the modified triangulation/multilateration procedure utilises the strain wave velocities propagation for impact positioning. The result shows that the finite element model can assist the experimental work for impact localisation in composite panel with less than 2 percent of total error per area.

1. Introduction

The use of composite materials has been widely accepted in many engineering applications. The high strength-to-weight ratio in composites is the main reason why these materials have regularly been chosen. Unfortunately, susceptibility of composite materials to impact damage has led many researchers to study various aspects of composite materials [1-2]. In general, damage detection research can be divided into active and passive methods. Active

methods can be defined as the application of signal/stress waves through a sensor/probe at one position and sensed by another sensor at another position. The frequency applied at the point can go up to 10MHz level. An example for this method is Lamb wave inspection [3]. The passive methods can be defined as monitoring any perturbation of the signals or any characteristic that can lead to impact damage [4]. Several different approaches have been implemented for impact damage detection, including

techniques based on non-destructive testing (NDT) and structural health monitoring (SHM) techniques. These techniques employ passive or active approaches.

Impact damage detection can be used to estimate impact location and energy. Initial studies of acoustic waves produced by low-velocity impacts have been investigated in [5]. The estimation of impact location and energy/force can be obtained using advanced signal processing techniques. Several of the damage detection methods have been applied to characterise the damage location and classification. These include Artificial Neural Network (ANN), triangulation procedure, Genetic Algorithm (GA) and wavelet approach [6-8]. Some simulation and modelling studies of impact damage detection have also been performed [9-10]. The method utilised a structural model which was used to obtain dynamic responses for simulated impact locations. Therefore in this paper; the aim is to compare the impact location obtained from the simulated strain signal with the experimental works.

2. Methodology

2.1 Finite Element Modelling

This research has employs the commercial finite element (FE) software package *ANSYS 7.0* to develop a simple three-dimensional model of a metallic ball impacting a composite plate. In this model the ball is dropped onto the plate, as illustrated in Figure 1. The objective of this investigation is to model the propagation of strain waves in the composite plate resulting from the impact.

The impactor is a spherical steel ball of 15mm diameter whereas the target is a rectangular composite plate of 608mm × 304mm × 3mm. The material properties for the steel ball and the composite plate are given in Table 1. The graphite/epoxy composite plate consists of 16 plies with a ply sequence of [0/90/45/-45]_{2s}. A *SMART*

Layer[®] [11] of transducers was embedded between the uppermost and subsequent lamina of the plate. However, for simplicity this layer of transducers was not modelled in the current FE work.

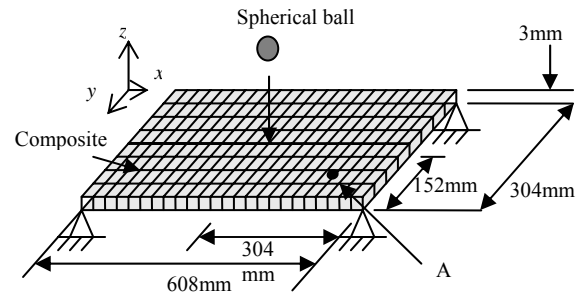


Figure 1: Illustration of FE impact modelling of the composite plate.

Table 1: Material properties of composite lamina and steel ball

Physical Properties	Lamina	Steel ball
Young Modulus [GPa]	$E_1 = 160.0$, $E_2 = E_3 = 8.9$	$E = 200$
Modulus of Rigidity [GPa]	$G_{12} = G_{13} =$ $G_{23} = 3.45$	$G = 77.5$
Poisson's ratio	$\nu_{12} = 0.28$	$\nu_{12} = 0.29$
Density [kg/m ³]	1545	7972

The *SHELL99* element was selected for the impact modelling work. It consists of 8 nodes with six degrees of freedom per node [12]. The composite plate was uniformly meshed with square shell elements of 4mm × 4mm, resulted in 23105 elements and 35113 nodes used in the model. Two other element types used in the impact modelling work were the *TARGE170* and *CONTA174* elements [12]. These elements modelled the impact event between the ball and the composite plate. The composite plate was simply supported at each corner. The transient loading was selected in the FE model that determines the

dynamic response of a structure under a time-varying load.

2.2 Genetic Algorithm with modified multilateration procedure

A genetic algorithm (GA) is an optimisation algorithm based on the principles of natural selection and natural genetics, developed in the 1970s by Holland [13]. GAs are designed to mimic natural biological evolution, i.e. inheritance, mutation, reproduction and crossover. GAs offer an alternative way to find optimal solutions close in performance to the global optimum (i.e. maximum or minimum) value.

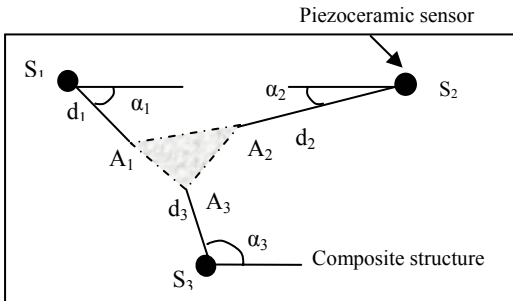


Figure 2: Illustration of the modified multilateration location procedure [7].

When an impact event occurs, the monitored structure deflects and strain waves propagate outwards in all possible directions; and the task is to estimate the position of this source. A modified multilateration procedure require three different transducers, labelled as S_1 , S_2 and S_3 , to detect these strain waves, as illustrated in Figure 2. The waves propagate from the unknown impact position towards these transducers. In the currently used impact location procedure, three different angles, α_1 , α_2 and α_3 , are randomly assumed for wave propagation directions. For every transducer S_i and assumed wave propagation angle α_i , the distance d_i between the transducer and the unknown impact position can be calculated as

$$d_i = v_i t_i \quad (i=1, 2, 3) \quad (1)$$

where t_i and v_i are the respective time-of-arrivals and velocities of the propagating strain waves. The t_i can be estimated from the experimental strain data for all relevant transducers. The major difficulty is that the velocity v_i depends on the wave propagation direction for anisotropic materials. However, the velocity characteristics $v_i = f(\alpha_i)$ can be estimated *a priori* for monitored composite structures using experimental analysis and/or FE modelling for all possible angles of wave propagation.

For the assumed wave propagation directions $\{\alpha_i\}$ and estimated distances $\{d_i\}$, the analysis of strain data from three different transducers results in three estimated impact positions, i.e. A_1 , A_2 and A_3 . These positions can be considered as vertices of a triangle. GA can then be used to minimise either the area or the total sum of all sides of this triangle. This finally leads to one estimate for the x and y coordinates of the unknown impact position.

3. Experimental Works

The finite element modelling results were experimentally validated. The focus was on the wave propagation velocities. A composite plate with the same dimensions and lay-up as the FE model was employed in this experiment. A *SMART[®] Layer* was embedded between the uppermost and subsequent lamina of the plate. This layer, manufactured by *Acellent Ltd*, constituted 12 piezoceramic transducers (6.5mm diameter and 0.25mm thickness) on a Kapton circuited layer. Figure 3 gives the impact and transducer positions. An impact hammer was used to produce impacts. The *LeCroy Waverunner LT-264* oscilloscope was used to capture and display all strain data from the impact events with a sampling frequency of 5

kHz. The experimental setup is shown in Figure 4.

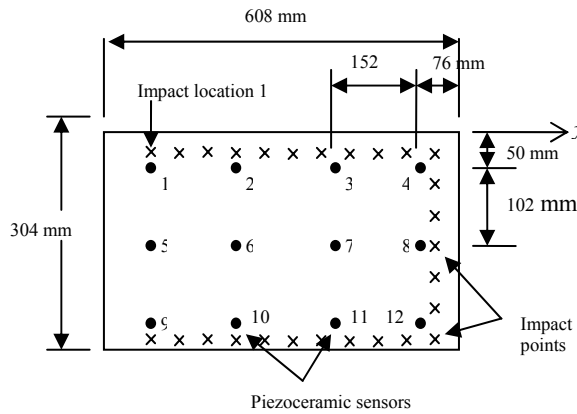


Figure 3: A composite plate embedded with 12 piezoceramic sensors

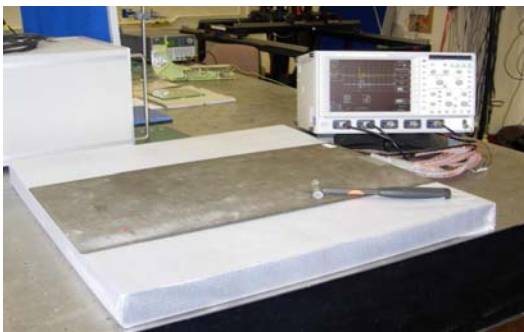


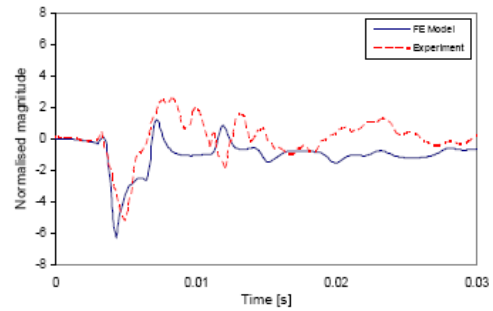
Figure 4: Experimental setup for low-velocity impacts on the composite plate

4. Results and Discussion

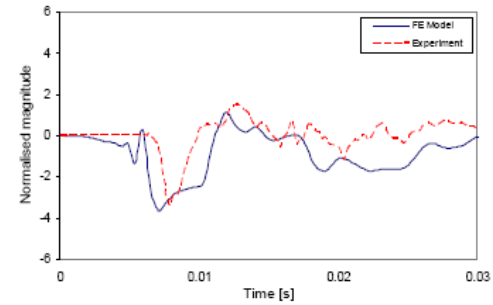
Figure 5 shows a comparison between the normalised simulated and experimental results. A zero-mean type of normalisation was used in this measurement. The calculation of data normalisation is as follow:

$$\hat{x}_i = \frac{x_i - \mu_i}{\sigma_i} \quad (2)$$

where \hat{x}_i is the normalised data, x_i is the i -th component of the original data, μ_i and σ_i are the mean and standard deviation of the original data respectively.



(a)



(b)

Figure 5: Comparison between the FE and experimental results for: (a) sensor 5 ($x=76$ mm, $y=152$ mm), (b) sensor 12 ($x=532$ mm, $y=252$ mm).

Although the experimental strain waves and FE modelling results do not exactly match, the shape of both waves is similar. In fact, the arrival times for the local impact minimum peak differ only by 9.5% and 12% respectively (the FE strain waves propagate faster than the experimentally-measured strain waves). It is thought that discrepancies could be due to the *SMART[®] Layer* not being modelled in the FE simulation work. Also, the boundary conditions applied to the composite plate in the FE model could be different from those actually occurring in the experimental case.

Figure 6 shows the comparison between the experimental and FE wave velocity characteristics. The experiment confirms that the wave velocity depends nonlinearly on the wave propagation direction. However, the results show that the waves obtained experimentally travel slower

than the simulated strain waves. This is in agreement with the first experiment performed in this section

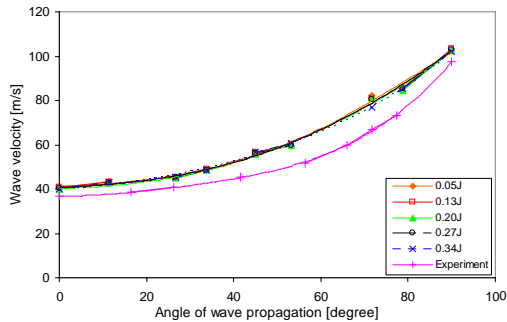


Figure 6: Wave velocity characteristics – comparison between the experimental and FE results

The impact location technique based on the modified multilateration procedure requires wave velocity characteristics from 0^0 to 360^0 . Therefore the experimental and FE wave velocity characteristics for the $0-90^0$ angle range were mirrored to produce the same characteristics for the 0^0-360^0 angle range, presented in Figure 7.

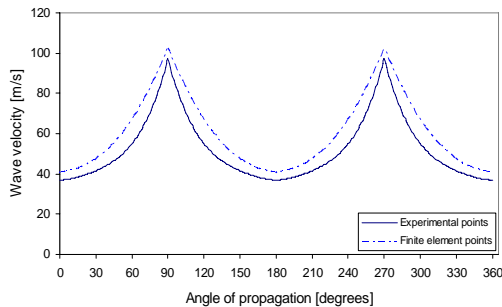
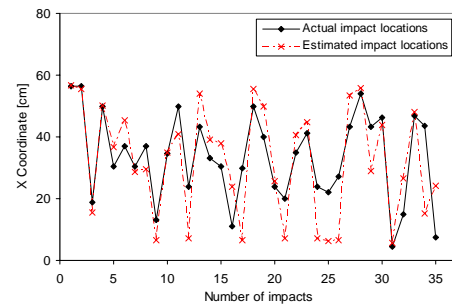
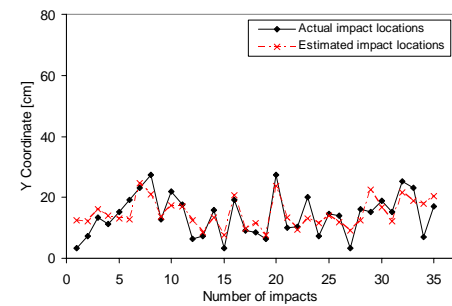


Figure 7: Wave velocity characteristics for the $0-360^0$ angle range of wave propagation,

Impact location results are given in Figure 8 and Figure 9. These two figures results compare the actual impact locations and estimated impact locations in terms of their x and y coordinate, respectively. The experimental wave velocity characteristic was used for impact location in Figure 8, whereas the FE-modelled wave velocity characteristic was used in Figure 9.

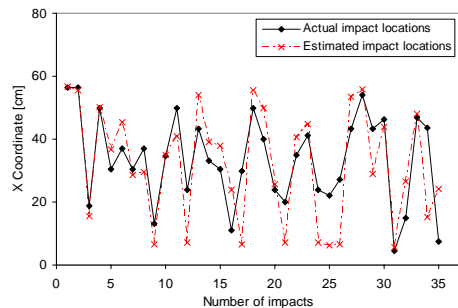


(a)

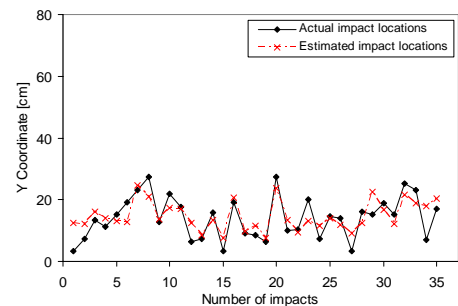


(b)

Figure 8: Impact location estimation based on the experimental wave velocity characteristic: (a) x coordinate (b) y coordinate.



(a)



(b)

Figure 9: Impact location based on the FE wave velocity characteristic: (a) x coordinate (b) y coordinate.

These results show that although the overall trends of the actual location curves are followed by the estimated location curves, there exist discrepancies in x and y coordinate estimates. The difference between the actual and estimated impact coordinates was calculated as an average distance. The percentage error of average distance per axis can be calculated as

$$E_s(x) = \frac{\sum_{i=1}^N |\hat{x}_i - x_i|}{(N) \times x_p} \times 100\% \quad (3)$$

$$E_s(y) = \frac{\sum_{i=1}^N |\hat{y}_i - y_i|}{(N) \times y_p} \times 100\% \quad (4)$$

where for a given total of N impacts on the composite structure, \hat{x} and \hat{y} are the predicted coordinates, x and y are the actual coordinates, and x_p and y_p are the size structure in the x and y coordinate axes.

The impact location performance was also assessed using a percentage error expressed in terms of the total area of the plate, given by

$$\varepsilon_A = \frac{\sum_{i=1}^N |\hat{x}_i - x_i| \times |\hat{y}_i - y_i|}{\text{area of structure} \times (N)^2} \times 100\% \quad (5)$$

Table 2 gives a summary of all the analysed errors. These results indicate that the GA-based algorithm has produced good estimates over the impact area. The maximum area error was less than 2% of the total area of the plate. It is also important to note that the FE-modelled wave velocity characteristics have given a relatively good performance if compared with the experimental wave velocity characteristics; their 1.72% error is only slightly larger than the 1.5% experimental error.

Table 2: Summary of analysed errors

	Exp	FE
Average error (x coordinate) [mm]	70.47	86.06
Average error (y coordinate) [mm]	39.36	36.84
Percentage error (x coordinate) [%]	11.59	14.15
Percentage error (y coordinate) [%]	12.95	12.11
Total error per analysed area [%]	1.50	1.72

5. Conclusion

Impact location of a composite plate was obtained with maximum area error was less than 2% of the total area. A good agreement between the experimental and simulated results was obtained in terms of wave propagation velocity, arrival time and nonlinear behaviour versus propagation direction. Strain data can be used together with the genetic algorithm in estimating the impact location. The simulated strain data from FE modelling can be used to simplify the analysis.

References

- [1] Z. Aslan, R. Karakuzu and B. Okutan, *Composite Structures*, 59, pp. 119-127, 2003
- [2] F.Mili and B. Necib, *Composite Structures*, 51, pp. 237-244, 2001.
- [3] S.S. Kessler, S.M. Spearing and C. Soutis, *Smart Materials and Structures*, 11, pp. 269-278, 2002
- [4] W.J. Staszewski, C. Biemans, C. Boller and G.R. Tomlinson, *Key Engineering Materials*, 221-222, pp. 389-400, 2002.
- [5] D. Weems, H.T. Hahn, E. Grandlund and I.G. Kim, *Proceedings of the 47th Annual Forum of the American Helicopter Society*, 1991.
- [6] K. Worden and W.J. Staszewski, *Strain*, 36, pp. 61-70, 2000
- [7] P.T. Coverley and W.J. Staszewski, *Smart Materials and Structures*, 12; pp. 1-9, 2003
- [8] Q.Wang and X.Deng, *Int. Journal of Solid and Structures*, 36; pp.3443-3468, 1999.
- [9] M. Tracy and F.K. Chang, *Journal of Intelligent Material Systems and Structures*, 9(11), pp. 920-928, 1998.

- [10] R. Seydel and F.K. Chang, *Smart Materials and Structures*; 10(2), pp. 354-369, 2001
- [11] F.K. Chang, *Proceedings of the 4th European Conference on Smart Materials and Structures, 2nd Int. Conf. on Micromechanics, Intelligent Materials and Robotics*, Harrogate, UK, pp. 771-781, 1998.
- [12] ANSYS: Release 6.1. Canonsburg, PA
- [13] D.E. Goldberg, *Genetic Algorithms in Search, Optimisation and Machine Learning*, Addison Wesley Publishing Co. Inc.